



OPEN Soy protein selectively accumulates formaldehyde

Masanori Yamada^{1✉}, Momoka Uchida¹ & Tetsuya Yamada²

Soy protein (SP) is easily obtained from defatted soybeans that have had soybean oil removed. Therefore, the materials consisting of soy protein are not only environmentally benign but also sustainable materials. We prepared the SP–GPTMS composite materials by mixing the SP and a silane coupling reagent, 3-glycidoxypyltrimethoxysilane (GPTMS), and demonstrated the accumulation of various aldehydes, such as formaldehyde (HAlD), acetaldehyde (AcAlD), butyl aldehyde (BuAlD), and benzaldehyde (BnAlD), by the SP–GPTMS composite materials. As a result, when the composite materials were incubated in an aqueous multi-component solution containing four aldehydes, these materials effectively accumulated the aldehydes. The accumulated amounts of the aldehydes were BnAlD < BuAlD < AcAlD < HAlD and the amount of HAlD was three times higher than that of BnAlD, which had the lowest accumulated amount. These results suggested that the SP–GPTMS composite materials indicated a molecular selectivity for HAlD. In addition, the accumulated amounts of HAlD further increased under acidic conditions. Furthermore, according to the IR measurements, the HAlD-accumulated SP–GPTMS composite materials showed the formation of Schiff base bonds. Therefore, the molecular selectivity of HAlD in the SP–GPTMS composite material was due to the high electrophilicity of HAlD and the low steric hindrance.

Keywords Soy protein, Formaldehyde, Selective accumulation, Aldehydes, Sustainable bio-resources

Aldehydes, such as formaldehyde (HAlD), acetaldehyde (AcAlD), butyl aldehyde (BuAlD), and benzaldehyde (BnAlD), have been used for solvents, synthetic reagents, fragrances, and preservatives around the world. Since these aldehydes easily react with various chemicals, many aldehyde species are undesirable or harmful to the human body and the natural environment^{1–4}. Especially, HAlD is utilized as the component of adhesives for gluing wallpaper and building materials. This HAlD component is slowly released from the wallpaper or the building material and causes a sick house syndrome⁵. Therefore, in Japan, the concentration of HAlD is strictly controlled under the Ordinance on Prevention of Hazards due to Specified Chemical Substances. Additionally, the World Health Organization (WHO) reported that HAlD possesses a carcinogenic property⁶. For these reasons, the materials for accumulating aldehydes, such as HAlD, in the air or water are important technology to maintain a healthy living environment⁷.

The accumulation of HAlD has been done using inorganic absorbents^{8–12}, such as activated carbon, zeolite, metal oxide, nanoporous materials, etc. In these cases, since inorganic absorbents accumulate HAlD based on physisorption, these materials can accumulate a lot of HAlD. However, inorganic absorbents do not have a molecular selectivity. Therefore, developments based on chemisorption are important. Generally, the amino group reacts with HAlD and forms Schiff base bonding^{13,14}. As a result, the amine group-immobilized inorganic materials have been used for the accumulation of HAlD¹⁵. In contrast, organic absorbents have also been reported as highly-porous polymer composites^{16–18}. Although these porous polymer materials can effectively accumulate the HAlD, these materials have to start with polymerizing the monomers. In addition, the raw material is petroleum and the accumulation of harmful compounds using an artificial polymer is not a sustainable technology. Therefore, the organic absorbents consisting of chitosan, foliage on tomato, and rush have also been reported^{19–21}. Recently, we also reported the accumulation of HAlD by a nucleic acid-inorganic hybrid material from an aqueous solution²². In this case, nucleic acids accumulated HAlD by reactions with the amino groups in the nucleobase, such as adenine, guanine, and cytosine. Additionally, the ribonucleic acid (RNA) accumulated HAlD more effectively than the deoxyribonucleic acid (DNA). Although the accumulations of HAlD by the nucleic acids or polysaccharides have been demonstrated, the accumulation of HAlD using protein has rarely been reported. Amino acids that have an amino group react with HAlD. However, since the amino acids are highly soluble in water, it is difficult to recover molecular amino acids that has reacted with HAlD from the solution. In contrast, since proteins, which are polymers of amino acids, have large molecular weight,

¹Department of Chemistry, Faculty of Science, Okayama University of Science, Ridaicho, Kita-ku, Okayama 700-0005, Japan. ²Graduate School of Agriculture, Hokkaido University, Kita 9, Nishi 9, Sapporo 060-8589, Hokkaido, Japan. ✉email: myamada@ous.ac.jp

proteins have lower solubility in water than amino acids. Therefore, materials consisting of protein are easier to recover from solution than amino acids, and these materials might be used as novel adsorbents for HAlD.

Soybean contains approximately 20% fat, 40% protein, and 20% carbohydrate by dried weight²³. The squeezed oil from soybean is used as cooking oils, industrial oils, and chemical reagents^{24–26}. Recently, the soy oil has also been used as soy ink, which does not use petroleum as a raw material. Since degreased soybeans contain a lot of proteins, soy protein (SP) has been consumed as a food for humans and a livestock feed. Additionally, degreased soybeans are also utilized as fertilizer. However, the amounts of degreased soybeans are too high to totally use and some degreased soybeans are discarded as industrial waste^{26,27}. In addition, the use of genetically modified soybeans in food raises many problems²⁸. Therefore, the utilization of SP is attractive from the viewpoint of sustainable chemistry and material science. The utilizations of SP have been reported as a hydrogel, adhesive, and UV-blocking agent^{26,29,30}. In addition, the SP is not only a low-cost material and environmentally benign, but it is also a biodegradable material. Therefore, we reported a novel bioplastic with a biodegradable property³¹. In this case, the SP formed a methylene cross-linking through the reaction of HAlD with basic amino acids, such as lysine and arginine that have amino groups in their side chains, and produced a biodegradable bioplastic. Since the SP has the ability to react with HAlD, the material consisting of SP would have the potential to accumulate various aldehydes.

In this study, we prepared SP–GPTMS composite materials by mixing the water-insoluble soy protein (SP) and a silane coupling reagent, 3-glycidoxypolytrimethoxysilane (GPTMS). This SP–GPTMS composite material was stable in water and rarely showed any swelling in water. When the SP–GPTMS composite materials were added to an aldehyde multi-component aqueous solution containing formaldehyde (HAlD), acetaldehyde (AcAlD), butyl aldehyde (BuAlD), and benzaldehyde (BnAlD), this material accumulated all the aldehydes. In addition, the accumulated amounts of the aldehydes were BnAlD < BuAlD < AcAlD < HAlD; the amount of HAlD was three times higher than that of BnAlD. These results suggested that the SP–GPTMS composite material exhibited a molecular selectivity for HAlD.

Experimental section

Material

The defatted soy protein and a silane coupling reagent 3-glycidoxypolytrimethoxysilane (GPTMS) were purchased from were purchased from Fujifilm Wako Pure Chemical Industries Ltd., Tokyo, Japan and Tokyo Kasei Industries, Tokyo, Japan, respectively. The GPTMS was used without the purification. Figure 1 shows the molecular structure of GPTMS. The formaldehyde (HAlD), acetaldehyde (AcAlD), butyl aldehyde (BuAlD), benzaldehyde (BnAlD), and azulene-1-carboxaldehyde (AzAlD) were obtained from Fujifilm Wako Pure Chemical Industries Ltd and Tokyo Kasei Industries. The molecular structures of HAlD, AcAlD, BuAlD, BnAlD, AzAlD are shown in Fig. 2. The 2,4-dinitrophenylhydrazine (DNPH) and 2-(N-morpholino)ethanesulfonic acid (MES) were also purchased from Fujifilm Wako Pure Chemical Industries Ltd. In all of the experiments, analytical grade reagents were used as organic solvents. Ultra-pure water (Merck KGaA, Darmstadt, Germany) was used in this experiment.

Preparation of SP–GPTMS composite material

The water-insoluble defatted SP was prepared as follows: purchased soy protein was dissolved in water (0.1 g ml^{−1}) and stirred overnight at room temperature. The SP solution was then centrifuged at 3500 rpm for 2 min and the supernatant containing the water-soluble SP was removed. After adding water to this sample, it was stirred and centrifuged to remove the water-soluble components. This processing was repeated three times. The obtained suspension of the water-insoluble SP was freeze-dried for 2 days or more.

The SP–GPTMS composite material was prepared as follows: the SP was first suspended in water (50 mg ml^{−1}). The GPTMS solution was added to the suspension of SP and immediately mixed by a vortex mixer. The concentration of GPTMS was 5 wt% relative to SP. This mixed solution was cast on a polytetrafluoroethylene (PTFE) plate and reacted at 140 °C for 20 min. This material was immersed in water for 1 h to remove the water-soluble components, then used in the further experiments.

Staining of SP–GPTMS composite material by azulene-1-carboxaldehyde (AzAlD)

The staining of the SP–GPTMS composite material by AzAlD was demonstrated as follows: the AzAlD was dissolved in a water-ethanol (1:1, v/v) mixed solution. The initial concentration of AzAlD was 15 mmol L^{−1}. The SP–GPTMS composite material was immersed in this AzAlD solution for 24 h. The AzAlD-accumulated SP–GPTMS composite material was then immersed in ethanol for more than 1 h to remove the non-accumulated AzAlD and rinsed several times with ethanol.

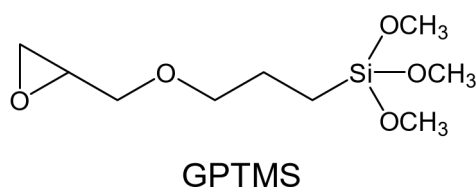


Fig. 1. Molecular structure of 3-glycidoxypolytrimethoxysilane (GPTMS).

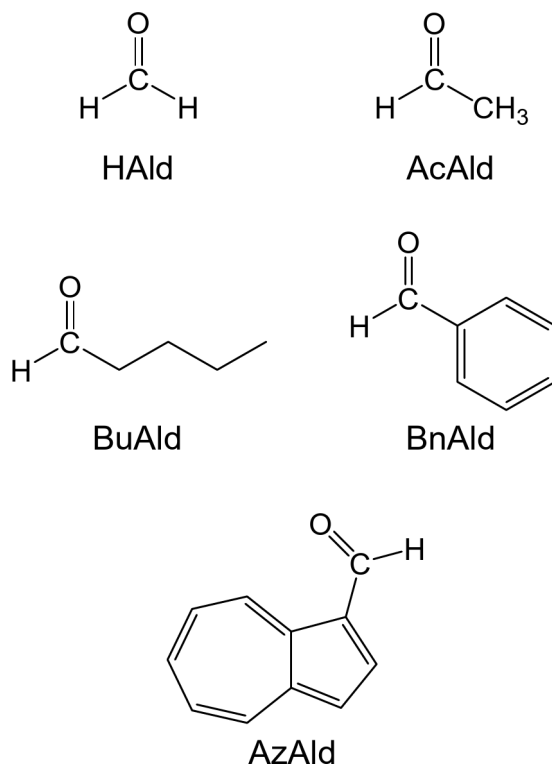


Fig. 2. Molecular structures of formaldehyde (HAlD), acetaldehyde (AcAld), butyl aldehyde (BuAld), benzaldehyde (BnAld), and azulene-1-carboxaldehyde (AzAld).

Measurements of swelling ratio

The swelling ratios of the SP–GPTMS composite material were measured as follows: the mass of the dried SP–GPTMS composite material was measured by a precious balance. This SP–GPTMS composite material was immersed in a water-ethanol (v/v) mixed solution for 1 h. The concentrations of ethanol were 0–100%. The mass of the immersed SP–GPTMS composite material was then immediately measured one more time. The swelling ratio was calculated using Eq. (1).

$$\text{Swelling ratio} = (\text{mass of immersed material}) / (\text{mass of dried material}) \quad (1)$$

where (mass of dried material) is the weight of the dried SP–GPTMS composite material before the immersion, while (mass of immersed material) is the weight of the immersed SP–GPTMS composite material after immersion in the water-ethanol mixed solution.

Accumulation of aldehydes by the SP–GPTMS composite material

The accumulation of aldehydes was demonstrated as follows: each HAlD, AcAld, BuAld, and BnAld was dissolved in ultrapure water (pH 7.0) or a 50 mM MES buffer solution (pH 5.5). Five SP–GPTMS composite materials were added to each of the aqueous aldehyde solutions (10 mL) which were stirred at room temperature for 1–24 h. The concentrations of the aldehydes were determined by the DNPH method³³. The colored solutions were analyzed by reverse-phase high performance liquid chromatography (HPLC) using an Inertsil[®] ODS-P column (7.6 × 250 mm, GL Science, Inc., Tokyo, Japan) with the isocratic elution mode. The eluent was methanol-water (80 : 20, v/v) and fed using a PCS Dual Pump SP-21 (Flom, Inc., Tokyo, Japan). The aldehydes were detected by an absorption at 360 nm using a UV-8010 UV-Vis detector (Tosoh Coop., Tokyo, Japan). The accumulated amounts of the aldehydes were calculated from the ratio of the peak area in the absence and presence of the SP–GPTMS composite materials.

The aqueous multi-component solution, which contained HAlD, AcAld, BuAld, and BnAld, was prepared by mixing these aldehydes. The concentrations of the four aldehydes were the same. The accumulation of the aldehydes was demonstrated using a procedure similar to that already described.

IR measurements of the aldehyde-accumulated SP–GPTMS composite material

The aldehyde-accumulated SP–GPTMS composite material was prepared as follows²²; the SP–GPTMS composite material was immersed in an aqueous HAlD solution at room temperature for 24 h. These samples were rinsed with water several times and dried overnight on a PTFE plate at room temperature. The concentration of HAlD was 0–8000 ppm. The IR spectra were measured using an FT/IR-4700 infrared spectrophotometer (JASCO Corporation, Tokyo, Japan) equipped with a diamond ATR prism.

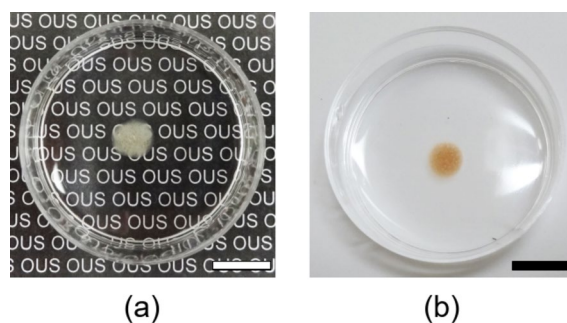


Fig. 3. Photographs of (a) SP-GPTMS composite material in water and (b) AzAld-accumulated SP-GPTMS composite material in ethanol. Each scale bar represents 10 mm.

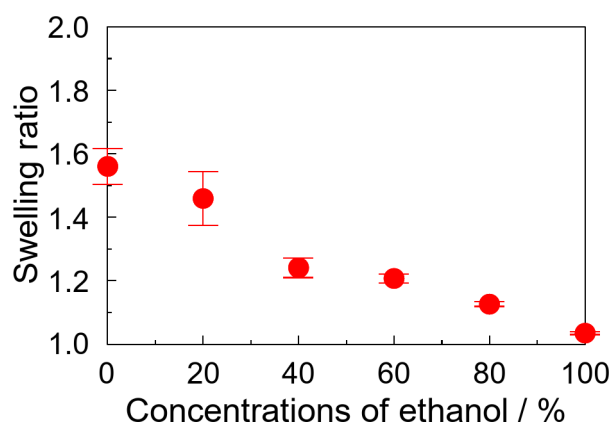


Fig. 4. The swelling ratios of the SP-GPTMS composite material in a water-ethanol (v/v) mixed solution. The swelling ratios were calculated using Eq. (1). The ethanol concentrations were 0–100%. Each of the values represents the mean of three separate determinations \pm standard deviations.

Results and discussion

Preparation of the SP-GPTMS composite material

The water-insoluble soy protein (SP) material without the addition of the silane coupling reagent, 3-glycidoxypolytrimethoxysilane (GPTMS), was prepared by casting of the suspended aqueous SP solution. Although the obtained SP material did not dissolve in water, it collapsed in the water. Additionally, the SP material could not be removed from the aqueous solution by pinching it with tweezers. These phenomena mean that the harmful compounds-accumulated SP materials are not easy to separate from aqueous solutions. Therefore, the SP material without the addition of GPTMS is not suitable for an absorbent. Thus, we prepared the SP-GPTMS composite material by the addition of GPTMS. The concentration of GPTMS was 5 wt% relative to SP. This SP-GPTMS composite material did not dissolve in water and could be pinched by the tweezers. This is due to the formation of organic-inorganic composite where organic and inorganic chains interact and the creation of new physical properties through compositing has been reported for various materials^{32,34–36}. Figure 3(a) shows a photograph of the SP-GPTMS composite material in water. This composite material was entirely translucent. In addition, this material was inflexible, hard, and brittle. Therefore, we evaluated the swelling ratio of the SP-GPTMS composite material in the water-ethanol (v/v) mixed solution.

Figure 4 shows the swelling ratio of the SP-GPTMS composite material in the water-ethanol (v/v) mixed solution. The concentrations of the ethanol were 0–100%. The swelling ratio was calculated using Eq. (1). When the SP-GPTMS composite material was immersed in water (0% ethanol), the swelling ratio was approximately 1.6. This value decreased with the increase in the ethanol concentration. Especially, at 100% ethanol (0% water), the swelling ratio was 1.03 and the composite material did not show any swelling. Since SP contained many hydrophilic amino acids in its structure³⁷, the SP-GPTMS composite material showed swelling with a high proportion of water. In contrast, SP did not interact with the ethanol and did not show any swelling. Since the accumulation of harmful compounds occurs due to their penetration into materials and their reaction with the compounds, materials that swell slightly in water could be used as absorbents for aldehydes. Therefore, we used the SP-GPTMS composite material as an accumulative material of aldehydes.

Staining of the SP-GPTMS composite material by azald

To visually evaluate the accumulation of aldehydes, we demonstrated the staining of the SP-GPTMS composite material by azulene-1-carboxaldehyde (AzAld). Although the azulene showed a different color depending on the

position of the substituent^{38,39}, the AzAld is reddish purple in a water-ethanol (1:1, v/v) mixed solution. When the SP–GPTMS composite material was immersed in a 15 mM AzAld solution, the milky white composite material became colored during the incubation time and changed to a reddish purple after 24 h. Figure 3(b) shows a photograph of the AzAld-accumulated SP–GPTMS composite material in ethanol. This is due to the accumulation of formyl group-immobilized azulene by the chemical interaction, and as a result, the AzAld-accumulated SP–GPTMS composite material became reddish purple. In addition, the composite material was dyed internally as well as on the surface. In contrast, since the AzAld is highly soluble in ethanol, the AzAld-accumulated SP–GPTMS composite material was immersed in ethanol for more than 24 h. However, the AzAld-accumulated SP–GPTMS composite material did not show any release of AzAld in ethanol. These results suggested that the SP–GPTMS composite material possessed the accumulative property of aldehydes via strong bonding, such as a chemical bonding. Therefore, we demonstrated the accumulation of aldehydes from an aldehyde-containing aqueous solution using a SP–GPTMS composite material.

Accumulation of aldehyde by then SP–GPTMS composite material using a single-component solution

The accumulations of aldehydes were demonstrated by immersing the SP–GPTMS composite material into each aqueous aldehyde solution. The aldehydes were used formaldehyde (HAld), acetaldehyde (AcAld), butyl aldehyde (BuAld), and benzaldehyde (BnAld). The coloring of the aldehydes was done by the DNPH method. The colored aldehyde solutions were analyzed by reverse-phase HPLC. The accumulated amounts of the aldehydes were calculated from the ratio of the peak area in the absence and presence of the SP–GPTMS composite material.

First, the accumulation time of the aldehydes by the SP–GPTMS composite material was evaluated. Figure 5 shows the accumulated amount of (closed circle) HAld, (closed square) AcAld, (closed triangle) BuAld, and (closed diamond) BnAld at various incubation times. The accumulated amount of HAld increased with the incubation time and reached a constant value at 6 h (see (closed circle) in Fig. 5). The constant value of HAld was approximately 0.3 μmol . A similar behavior was also obtained for other aldehydes, such as AcAld, BuAld, and BnAld, and showed a constant value at 6 h. Therefore, the accumulative measurements of the aldehydes were done at 6 h.

Figure 6 shows the accumulated amount of (closed circle) HAld, (closed square) AcAld, (closed triangle) BuAld, and (closed diamond) BnAld in an aqueous solution for various concentrations. The accumulated amount of HAld increased with the initial concentration and reached a constant value at ca. 2.9 μmol (see (closed circle) in Fig. 6). Therefore, we defined the constant value as the maximum accumulated amount of the aldehydes. Similar phenomena were obtained for the other aldehydes, such as AcAld, BuAld, and BnAld, and the maximum accumulated amounts of AcAld, BuAld, and BnAld were 2.5 μmol , 1.4 μmol , and 1.0 μmol , respectively. The green bars in Fig. 7 shows the maximum accumulated amounts of HAld, AcAld, BuAld, and BnAld in an aqueous single-component solution. As a result, the SP–GPTMS composite material accumulated the most HAld. The maximum accumulated amount of HAld was almost three times that of BnAld, which had the lowest accumulated amount. Therefore, we demonstrated the accumulation from the multi-component solution.

Accumulation of aldehyde by the SP–GPTMS composite material using a multi-component solution

An aqueous multi-component solution was prepared by mixing the HAld, AcAld, BuAld, and BnAld. The concentration of each aldehyde was the same and the incubation time was 6 h. Figure 8 shows the accumulated amounts of (closed circle) HAld, (closed square) AcAld, (closed triangle) BuAld, and (closed diamond) BnAld from the multi-component solution. The accumulated amount of HAld increased with the initial concentration

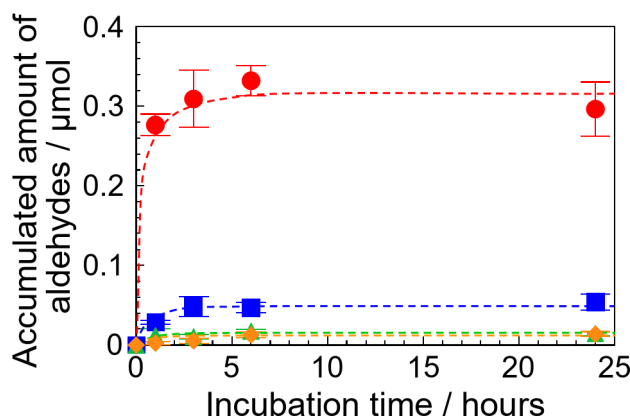


Fig. 5. Accumulated amounts of (closed circle) HAld, (closed square) AcAld, (closed triangle) BuAld, and (closed diamond) BnAld by the SP–GPTMS composite material in an aqueous single-component solution for various incubation times. Each concentration of the aldehydes was 1 ppm. Each of the values represents the mean of three separate determinations \pm standard deviations.

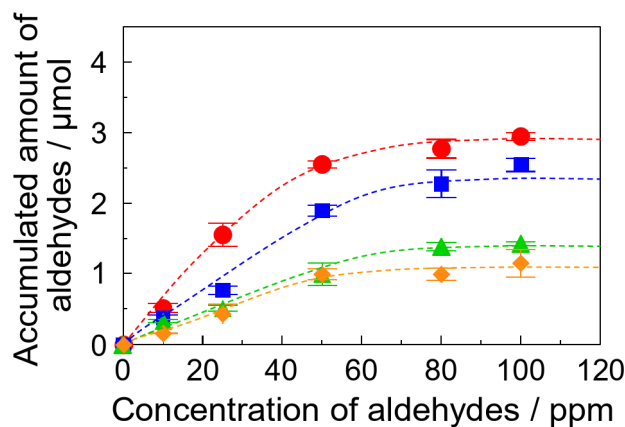


Fig. 6. Accumulated amounts of (closed circle) HAlD, (closed square) AcAlD, (closed triangle) BuAlD, and (closed diamond) BnAlD by the SP – GPTMS composite material in an aqueous single-component solution for various concentrations. The incubation time was 6 h. Each of the values represents the mean of three separate determinations \pm standard deviations.

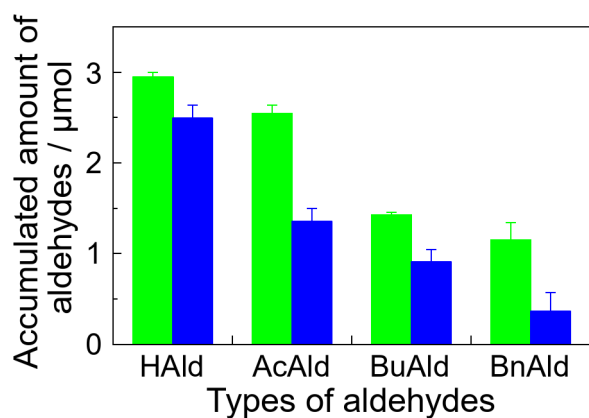


Fig. 7. Maximum accumulated amounts of HAlD, AcAlD, BuAlD, and BnAlD in (green bars) aqueous single-component solution and (blue bars) aqueous multi-components solution. Error bars showed standard deviations.

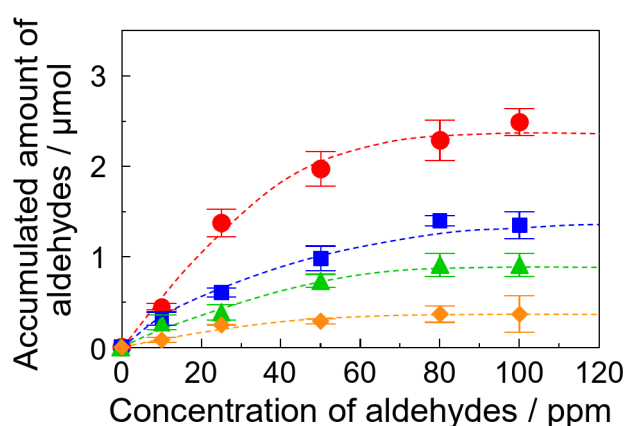


Fig. 8. Accumulated amounts of (closed circle) HAlD, (closed square) AcAlD, (closed triangle) BuAlD, and (closed diamond) BnAlD by the SP – GPTMS composite material in an aqueous multi-components solution for various concentrations. The incubation time was 6 h. Each of the values represents the mean of three separate determinations \pm standard deviations.

and reached a constant value (see (closed circle) in Fig. 8). Similar behaviors were also obtained for the other aldehydes. The maximum accumulated amounts of HALd, AcAld, BuAld, and BnAld were 2.5 μmol , 1.3 μmol , 0.9 μmol , and 0.4 μmol , respectively. For the accumulation of aldehydes from a multi-component solution, the accumulated amount of HALd was almost five times higher than that of BnAld, which had the lowest accumulated amount. As a result, the selectivity of the aldehydes was $\text{BnAld} < \text{BuAld} < \text{AcAld} < \text{HALd}$, thus the SP–GPTMS composite material showed the highest selectivity for HALd. The blue bars in Fig. 7 show the maximum accumulated amounts of the aldehydes in an aqueous multi-components solution. The accumulated amount of the aldehydes from an aqueous multi-components solution was lower than that from the single-components. This is because the number of accumulative sites decreased by using four aldehydes. These results suggested that the SP–GPTMS composite materials could selectively accumulate the HALd even in an aqueous multi-component solution. Therefore, we evaluated the accumulative mechanism of HALd in the SP–GPTMS composite materials using infrared spectroscopy.

IR spectra of the HALd-accumulated SP–GPTMS composite material

Figure 9(a)–(c) shows the IR spectra in the 800–1800 cm^{-1} region of the HALd-accumulated SP–GPTMS composite material incubated at the concentrations of 0 ppm (no HALd in water), 4000 ppm, and 8000 ppm. The SP–GPTMS composite material without the accumulation of HALd showed absorption bands at 1076 cm^{-1} and 1045 cm^{-1} related to the stretching vibration of C–N in the primary amine and secondary amine^{40,41}, respectively. When the concentration of HALd increased, the intensity of the absorption band at 1076 cm^{-1} decreased. In addition, the intensity of the absorption band at 1045 cm^{-1} increased with the concentration of HALd. Furthermore, the absorption band at 1058 cm^{-1} , attributed to =C–H, appeared at the high HALd concentrations, such as 8000 ppm. These phenomena, such as the appearance of an absorption band related to Schiff base bonds, have been reported for the reaction of chitosan and vanillin derivative¹⁴. These results suggested that the HALd reacted with the primary amines in SP and produced the Schiff base bonds. In contrast, since the Schiff base forms C=N, the absorption band of C=N at approximately 1600 cm^{-1} appears. However, these IR spectra in Fig. 9 did not show this absorption band due to the strong absorption of amide bonds.

In general, the efficiency of these reactions, such as the amine and HALd, depends on the pH conditions. Especially, under acidic conditions, the electrophilicity of the carbon atom in HALd increases by the addition of a proton to the oxygen atom⁴². Therefore, we demonstrated the accumulation of HALd under acidic conditions.

Accumulation of the aldehyde by SP–GPTMS composite material under acidic conditions

The red bar in Fig. 10 show the maximum accumulated amount of HALd from a single-component solution under the pH 5.5 conditions. The maximum accumulated amounts at pH 7.0 are reshown as the blue bar in Fig. 10. The accumulated amount of HALd at pH 5.5 was 5.2 μmol and this value was approximately 1.8 times the accumulated amount at pH 7.0. The increases in the accumulated amount were also obtained for the other aldehydes, such as AcAld, BuAld, and BnAld. However, the increased ratios of the accumulated amounts under the pH 5.5 conditions were lower than that of HALd. In contrast, similar results were also obtained for the multi-component solution (see insert in Fig. 10). Furthermore, the selectivity of the aldehydes was $\text{BnAld} < \text{BuAld} < \text{AcAld} < \text{HALd}$.

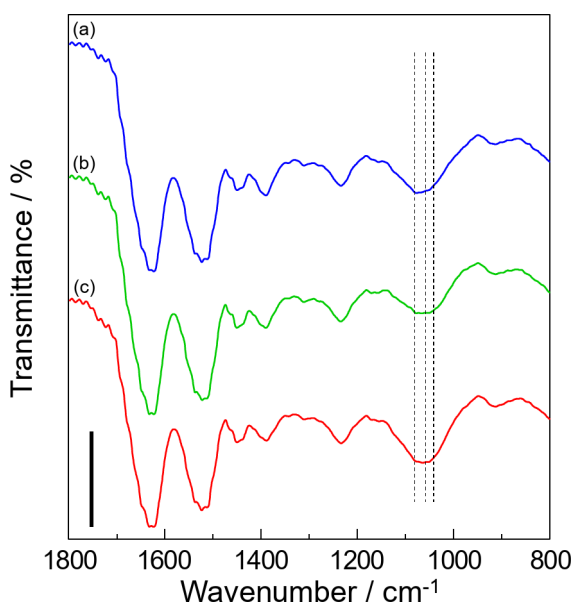


Fig. 9. IR spectra in 800–1800 cm^{-1} region of HALd-accumulated SP–GPTMS composite material. The concentrations of the aqueous HALd solution are (a) 0 ppm (no HALd in water), (b) 4000 ppm, and (c) 8000 ppm. The dashed lines are the 1076 cm^{-1} , 1058 cm^{-1} , and 1045 cm^{-1} peaks. The scale bar indicates a transmittance of 10%. Similar results were obtained for the triplicate experiments.

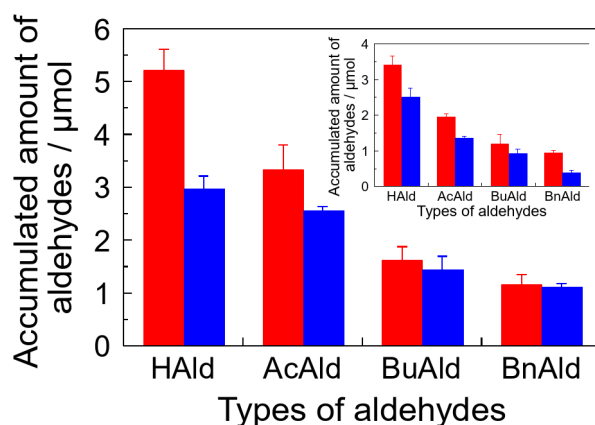


Fig. 10. Maximum accumulated amounts of HAlD, AcAlD, BuAlD, and BnAlD from an aqueous single-component solution at pH 5.5 (red bars) and pH 7.0 (blue bars). The insert in the figure shows the accumulated maximum amounts from an aqueous multi-component solution at pH 5.5 (red bars) and pH 7.0 (blue bars). Error bars showed standard deviations.

Materials	Adsorption capacity / mg g^{-1}	Ref.
Ground kaolin	3.41	43
Bentonite	5.03	43
Zeolite	0.393	44
Activated carbon	19.86	45
Activated carbon fibre	14.3	46
Ag modified activated carbon	<120	47
Reduced graphene oxide-polymer	140	18
Chitosan grafted cyclodextrin	15.5	48
Modified poly(aspartic acid)	23.87	49
Chitosan aerogel beads	66	50
RNA-inorganic hybrid material	2.9	22
Soy protein	6.2	this work

Table 1. The adsorption capacity of HAlD by the HAlD-absorbent material and the SP–GPTMS composite material.

The reactivity of the aldehydes is based on the electrophilicity of the carbon in the carbonyl group. Under acidic conditions, the electrophilicity increases due to the addition of protons to the oxygen atoms. In contrast, although the methyl group in AcAlD and the butyl group in BuAlD act as electron-withdrawing groups, the phenyl groups in BnAlD behave as electro-donating groups. As a result, BnAlD exhibits the lowest electrophilicity of the four aldehydes. In addition, the steric hindrances of the functional groups in the aldehydes are $\text{HAlD} < \text{AcAlD} < \text{BuAlD} < \text{BnAlD}$. Since the bulky functional groups inhibit the reaction with the basic amino acids in SP, the accumulated amounts of the aldehydes with the high steric hindrance, such as BnAlD, decreased. Therefore, the SP–GPTMS composite material selectively accumulated HAlD from an aldehyde-containing aqueous solution.

Comparison of HAlD absorption capacity of SP–GPTMS composite material and other HAlD-absorbent materials

Finally, we compared the HAlD accumulation of SP–GPTMS composite material and other HAlD-absorbent materials. Table 1 shows the absorption capacity of HAlD by the HAlD-absorbent materials and the SP–GPTMS composite material. The activated carbon and their related substrates showed the high absorption capacity. Therefore, the various HAlD-absorbent materials based on activated carbon have been reported^{8,9}. In addition, aerogel and porous polymer materials showed high adsorption capacity. Especially, the reduced graphene oxide-templated polymer composites indicate high adsorption capacity for removal of gaseous HAlD under ambient conditions¹⁸. On the other hand, the adsorption capacity of SP–GPTMS composite material was ca. 6 mg g^{-1} and this value was slightly higher than that of natural minerals, such as bentonite and kaolin. The SP–GPTMS composite material is consisting of protein, which is low cost natural polymer. Additionally, this composite material was prepared by simply mixing the protein and a silane coupling reagent. Therefore, the SP–GPTMS composite material is low cost not only raw materials but also the synthesis process. In nature, there are proteins

that contain a lot of arginine and lysine, which can react with HCHO. By using such proteins, it will be possible to create petroleum-free materials with even higher adsorption capacity of HAlD.

Conclusion

We prepared SP–GPTMS composite materials by mixing the water-insoluble soy protein (SP) and a silane coupling reagent, 3-glycidoxypolytrimethoxysilane (GPTMS). When the composite materials were immersed in an azulene-1-carboxaldehyde (AzAld) solution, the composite material showed a reddish-purple color due to the accumulation of AzAld by the reaction of the formyl and amino groups. Therefore, we demonstrated the accumulation of various aldehydes by using the composite material. When the SP–GPTMS composite materials were added to an aldehyde multi-components aqueous solution containing formaldehyde (HAlD), acetaldehyde (AcAld), butyl aldehyde (BuAld), and benzaldehyde (BnAld), the composite material accumulated all the aldehydes. In addition, the accumulated amounts increased under the acidic conditions. Furthermore, these accumulated amounts were BnAld < BuAld < AcAld < HAlD and the composite material showed a high molecular selectivity for HAlD. This was due to the high electrophilicity of HAlD and the low steric hindrance. The SP–GPTMS composite material consisting of sustainable resources is environmentally benign. Therefore, these materials have a potential for accumulating formaldehyde from industrial wastewater, experimental wastewater, and river water. Furthermore, these materials might be used for the removal of harmful compounds from the human body.

Data availability

All data that supports the findings of this study is available within the article.

Received: 27 February 2024; Accepted: 3 March 2025

Published online: 18 March 2025

References

1. Salthammer, T., Mentese, S. & Marutzky, R. Formaldehyde in the indoor environment. *Chem. Rev.* **110**, 2536–2572 (2010).
2. Zhang, L. *Formaldehyde: exposure, toxicity and health effects* The Royal Society of Chemistry, (2018). <https://doi.org/10.1039/9781788010269-00001>
3. McLaughlin, J. K. Formaldehyde and cancer: a critical review. *Int. Arch. Occup. Environ. Health.* **66**, 295–301 (1994).
4. Barbour, A. K. et al. *Air Pollution and Health* (The Royal Society of Chemistry, 1998). <https://doi.org/10.1039/9781847550095>
5. Sick building syndrome, World Health Organization Regional Office for Europe. https://www.aivc.org/sites/default/files/members_area/medias/pdf/Inive/ECA/ECA_Report4.pdf (accessed 2024-01-01).
6. IARC Formaldehyde, 2-butoxyethanol and 1-tert-butoxypropan-2-ol. *IARC Monogr. Eval. Carcinog. Risks Hum.* **88**, 1–478 (2006).
7. Robert, B. & Nallathambi, G. Indoor formaldehyde removal by catalytic oxidation, adsorption and nanofibrous membranes: a review. *Environ. Chem. Lett.* **19**, 2551–2579 (2021).
8. Kang, Y. J. et al. I. A brief review of formaldehyde removal through activated carbon adsorption. *Appl. Sci.* **12**, 5025 (2022). (15 pages).
9. Suresh, S. & Bandosz, T. J. Removal of formaldehyde on carbon-based materials: a review of the recent approaches and findings. *Carbon* **137**, 207–221 (2018).
10. Bellata, J. P. et al. Capture of formaldehyde by adsorption on nanoporous materials. *J. Hazard. Mater.* **300**, 711–717 (2015).
11. Shiraishi, F., Yamaguchi, S. & Ohbuchi, Y. A rapid treatment of formaldehyde in a highly tight room using a photocatalytic reactor combined with a continuous adsorption and desorption apparatus. *Chem. Eng. Sci.* **58**, 929–934 (2003).
12. Truong, C. M., Wu, M. C. & Goodman, D. W. Adsorption of formaldehyde on nickel oxide studied by thermal programmed desorption and high-resolution electron energy loss spectroscopy. *J. Am. Chem. Soc.* **115**, 3647–3653 (1993).
13. Okunzuwa, G. I., Enaroseha, O. O. E. & Okunzuwa, S. I. Synthesis and characterization of Fe(III) Chitosan nanoparticles n-benzaldehyde schiff base for biomedical application. *Chem. Pap.* **78**, 3253–3260 (2024).
14. Zhu, J., Chen, X., Huang, T., Tian, D. & Gao, R. Characterization and antioxidant properties of chitosan/ethyl-vanillin edible films produced via Schiff–base reaction. *Food Sci. Biotechnol.* **32**, 157–167 (2023).
15. Photong, S. & Boonamnuyvitaya, V. Synthesis of APTMS-functionalized SiO₂/TiO₂ transparent film using Peroxo titanic acid refluxed solution for formaldehyde removal. *Water Air Soil. Pollut.* **210**, 453–461 (2010).
16. Sun, T., Lai, Y., Ye, L. & Zhao, X. A new and highly efficient formaldehyde absorbent of polyoxymethylene. *Polym. Adv. Technol.* **19**, 1286–1295 (2008).
17. Na, C. J., Yoo, M. J., Tsang, D. C. W., Kim, H. W. & Kim, K. H. High-performance materials for effective sorptive removal of formaldehyde in air. *J. Hazard. Mater.* **366**, 452–465 (2019).
18. Wang, L. et al. Zero-carbon emission chemical method to remove formaldehyde without catalyst by highly porous polymer composites at room temperature. *Macromol. Rapid Commun.* **44**, 2200629 (2023). (9 pages).
19. Nuasaena, S., Opaprakasit, P. & Tangboriboonrata, P. Hollow latex particles functionalized with Chitosan for the removal of formaldehyde from indoor air. *Carbohydr. Polym.* **101**, 179–187 (2014).
20. Kobayashi, T., Shiratake, K. & Tabuchi, T. Studies for absorption of formaldehyde by using foliage on wild tomato species. *Hort J.* **87**, 214–221 (2018).
21. Yamamoto, K., Aoyama, S. & Matsuura, T. Adsorption property of rush for formaldehyde. *Bull. Ind. Res. Inst. Hiroshima Prefecture East.* **16**, 92–94 (2003).
22. Yamada, M., Funaki, S. & Miki, S. Formaldehyde interacts with RNA rather than DNA: accumulation of formaldehyde by the RNA-inorganic hybrid material. *Int. J. Biol. Macromol.* **122**, 168–173 (2019).
23. El-Shemy, H. *Soybean bio-active Compounds* (IntechOpen Limited, 2013).
24. O’Toole, D. K. Characteristics and use of Okara, the soybean residue from soy milk productions: a review. *J. Agric. Food Chem.* **47**, 363–371 (1999).
25. Gu, W. et al. Recent progress in robust regenerated soy protein film. *Macromol. Mater. Eng.* **2300224**, 18pages (2023).
26. Visakh, P. M. & Nazarenko, O. *Soy protein-based Blends, Composites and Nanocomposites* (Wiley, 1998).
27. Tian, W. et al. Recent progress of biomass in conventional wood adhesives: a review. *Green. Chem.* **25**, 10304–10337 (2023).
28. Yadav, V., Pal, D. & Poonia, A. K. A study on genetically engineered foods: need, benefits, risk, and current knowledge. *Cell. Biochem. Biophys.* <https://doi.org/10.1007/s12013-024-01390-x> (2024).
29. Cuadri, A. A., Bengoechea, C., Romero, A. & Guerrero, A. A natural-based polymeric hydrogel based on functionalized soy protein. *Eur. Polym. J.* **85**, 164–174 (2016).
30. Lamaming, S. Z. et al. Improvements and limitation of soy protein-based adhesive: a review. *Polym. Eng. Sci.* **61**, 2393–2405 (2021).

31. Yamada, M., Morimitsu, S., Hosono, E. & Yamada, T. Preparation of bioplastic using soy protein. *Int. J. Biol. Macromol.* **149**, 1077–1083 (2020).
32. Yamada, M., Ujihara, M. & Yamada, T. The accumulation of metal ions by a soy protein–inorganic composite material. *J. Compos. Sci.* **7**, 419 (2023). (13 pages).
33. Salthammer, T. Acetaldehyde in the indoor environment. *Environ. Sci. : Atmos.* **3**, 474–493 (2023).
34. Samiey, B., Cheng, C. H. & Wu, J. Organic–inorganic hybrid polymers as adsorbents for removal of heavy metal ions from solutions: a review. *Materials* **7**, 673–726 (2014).
35. Sanchez, C., Julián, B., Belleville, P. & Popall, M. Applications of hybrid organic–inorganic nanocomposites. *J. Mater. Chem.* **15**, 3559–3592 (2005).
36. Pandey, S. & Mishra, S. B. Sol–gel derived organic–inorganic hybrid materials: synthesis, characterizations and applications. *J. Sol-Gel Sci. Technol.* **59**, 73–94 (2011).
37. Taira, H. Heat destruction of amino acids in soybean products. *Jpn Agric. Res. Q.* **7**, 267–273 (1973).
38. Hafner, K. & Bernhar, C. *Azulen-aldehyde Und -ketone* (Wiley-VCH, 1959).
39. Zeng, H. N., Png, Z. M. & Xu, J. Azulene in polymers and their properties. *Chem. Asian J.* **15**, 1904–1915 (2020).
40. Silverstein, R. M. & Webster, F. X. *Spectrometric Identification of Organic Compounds* (Wiley, 1998).
41. Stewart, J. E. Vibrational spectra of primary and secondary aliphatic amines. *J. Chem. Phys.* **30**, 1259–1265 (1959).
42. McMurry, J. *Organic Chemistry* (Cengage learning, 2015).
43. Salman, M., Athar, M., Shafique, U. & Rehman, R. Removal of formaldehyde from aqueous solution by adsorption on Kaolin and bentonite: a comparative study. *Turkish J. Eng. Environ. Sci.* **36**, 263–270 (2012).
44. Paliulis, D. Removal of formaldehyde from synthetic wastewater using natural and modified zeolites. *Pol. J. Environ. Stud.* **25**, 251–257 (2016).
45. Khaleghi, H., Esmaili, H., Jaafarzadeh, N. & Ramavandi, B. Date seed activated carbon decorated with CaO and Fe₃O₄ nanoparticles as a reusable sorbent for removal of formaldehyde. *Korean J. Chem. Eng.* **39**, 146–160 (2022).
46. Song, Y. et al. Removal of formaldehyde at low concentration using various activated carbon fibers. *J. Appl. Polym. Sci.* **106**, 2151–2157 (2007).
47. Wara, D. P. R., Wahyuni, S. & Feinnudin, A. Thermodynamics of formaldehyde removal by adsorption onto nanosilver loaded bamboo-based activated carbon. *Mater. Sci. Forum.* **890**, 93–97 (2017).
48. Yang, Z., Miao, H., Rui, Z. & Ji, H. Enhanced formaldehyde removal from air using fully biodegradable Chitosan grafted β -cyclodextrin adsorbent with weak chemical interaction. *Polymers* **11**, 276 (2019). (15 pages).
49. Zhang, Y. et al. Synthesis and characterization of modified poly(aspartic acid) and its performance as a formaldehyde adsorbent. *J. Appl. Polym. Sci.* **135**, 45798 (2017). (6 pages).
50. Wu, P. & Liu, Z. Chitosan aerogel beads with microfibrillated cellulose skeleton for removal of formaldehyde from indoor air. *Cellul Chem. Technol.* **51**, 521–528 (2017).

Author contributions

M.Y.: Conceptualization, Data curation, Formal analysis, Funding acquisition, Investigation, Methodology, Project administration, Resources, Software, supervision, Validation, Visualization, Writing – original draft, Writing – review & editing. M.U.: Formal analysis, Software. T.Y.: Conceptualization, Formal analysis. All authors reviewed the manuscript.

Funding

This work was supported by JSPS KAKENHI Grant Number JP22K12451.

Declarations

Competing interests

The authors declare no competing interests.

Additional information

Correspondence and requests for materials should be addressed to M.Y.

Reprints and permissions information is available at www.nature.com/reprints.

Publisher's note Springer Nature remains neutral with regard to jurisdictional claims in published maps and institutional affiliations.

Open Access This article is licensed under a Creative Commons Attribution-NonCommercial-NoDerivatives 4.0 International License, which permits any non-commercial use, sharing, distribution and reproduction in any medium or format, as long as you give appropriate credit to the original author(s) and the source, provide a link to the Creative Commons licence, and indicate if you modified the licensed material. You do not have permission under this licence to share adapted material derived from this article or parts of it. The images or other third party material in this article are included in the article's Creative Commons licence, unless indicated otherwise in a credit line to the material. If material is not included in the article's Creative Commons licence and your intended use is not permitted by statutory regulation or exceeds the permitted use, you will need to obtain permission directly from the copyright holder. To view a copy of this licence, visit <http://creativecommons.org/licenses/by-nc-nd/4.0/>.

© The Author(s) 2025